International Journal of Minerals, Metallurgy and Materials
Volume 20, Number 7, July 2013, Page 645
DOI: 10.1007/s12613-013-0778-4

Stress corrosion cracking of X80 pipeline steel exposed to high pH solutions with different concentrations of bicarbonate

Lin Fan, Cui-wei Du, Zhi-yong Liu, and Xiao-gang Li

School of Materials Science and Engineering, University of Science and Technology Beijing, Beijing 100083, China

(Received: 1 November 2012; revised: 15 March 2013; accepted: 17 March 2013)

Abstract: Susceptibilities to stress corrosion cracking (SCC) of X80 pipeline steel in high pH solutions with various concentrations of HCO_3^- at a passive potential of –0.2 V vs. SCE were investigated by slow strain rate tensile (SSRT) test. The SCC mechanism and the effect of HCO_3^- were discussed with the aid of electrochemical techniques. It is indicated that X80 steel shows enhanced susceptibility to SCC with the concentration of HCO_3^- increasing from 0.15 to 1.00 mol/L, and the susceptibility can be evaluated in terms of current density at –0.2 V vs. SCE. The SCC behavior is controlled by the dissolution-based mechanism in these circumstances. Increasing the concentration of HCO_3^- not only increases the risk of rupture of passive films but also promotes the anodic dissolution of crack tips. Besides, little susceptibility to SCC is found in dilute solution containing 0.05 mol/L HCO_3^- for X80 steel. This can be attributed to the inhibited repassivation of passive films, manifesting as a more intensive dissolution in the non-crack tip areas than at the crack tips.

Keywords: pipeline steel; stress corrosion cracking; bicarbonate; passive films

1. Introduction

Stress corrosion cracking (SCC), as a typical localized corrosion, is one of the most dangerous failure forms occurring in buried pipelines used for high-pressure natural gas transmission, which usually causes sudden leakage and rupture without awareness. This may affect the service safety of pipeline steels [1]. X80 pipeline steel is becoming one of the most widely applied pipe materials because of its high strength and toughness [2]. Although upgrading in steel-grade allows economic benefits and a better performance, this may sacrifice substantial SCC resistance [3].

According to Refs. [1,4], high pH SCC can be attributed primarily to a dissolution-based mechanism, i.e., crack propagation was facilitated by anodic dissolution and repeated rupture of passive films at the crack tips. Many researchers [5-7] believed that the resistance to SCC relied on the properties of passive films formed in concentrated carbonate/bicarbonate solutions. The rupture of passive films usually led to the occurrence of pitting [8-10], which was probably the main cause of initiation of SCC, especially under the application of anodic potentials [11].

Parkins and Zhou [12] found that SCC behavior could be influenced to some extent by the concentration of HCO_3^-, with the increase of crack growth rate as the concentration of HCO_3^- increased. Previous work of our research group [13-14] confirmed that the increase in HCO_3^- concentration deteriorated the corrosion resistance of passive films. However, the relationship between the SCC behavior of X80 pipeline steel and the rupture of passive films assisted by HCO_3^- in high pH solutions is still unknown. Furthermore, whether the SCC behavior follows the dissolution-based mechanism at passive potential needs verifying.

In light of this, susceptibilities to SCC of X80 pipeline steel in high pH solutions with various concentrations of HCO_3^- at a passive potential were investigated in this work by slow strain rate tensile (SSRT) test. Based on potentiodynamic polarization curves obtained at quick and slow sweep rates and electrochemical impedance spectroscopy (EIS) measurements, the relationship between the SCC behavior and the HCO_3^- assisted film rupture was discussed.

Corresponding author: Xiao-gang Li E-mail: lixiaogang99@263.net

2. Experimental

2.1. Specimens and solutions

Specimens used in this work were made of X80 pipeline steel supplied by Bao Steel Co. Ltd., with the chemical composition (wt%) of 0.036 C, 0.197 Si, 1.771 Mn, 0.012 P, 0.002 S, 0.223 Cr, 0.278 Ni, 0.220 Cu, 0.021 Al, 0.019 Ti, 0.184 Mo, 0.001 V, 0.110 Nb, 0.005 N, and Fe balance. Its yielding strength was 640 MPa and the ultimate tensile strength was 750 MPa. The specimens used in conventional electrochemical measurements were embedded in epoxy resin with the working area of 1.0 cm^2. For SSRT test, smooth flat tensile specimens were used with the gauge size of 36 mm in length, 6 mm in width, and 2 mm in thickness, in which the long axis of the specimens was parallel to the circumferential direction of the steel pipe. Prior to the test, all the specimens were ground from 60 grit up to 1000 grit silicon carbide paper, then rinsed with deionized water, and degreased in acetone. Bicarbonate solutions consisting of 0.05 mol/L NaCl and different concentrations of HCO_3^- (0.05-1.00 mol/L) were used as the testing solution, and the pH value of solution was kept at approximately 8.31.

2.2. Experimental methods

Susceptibilities to SCC of X80 pipeline steel were evaluated using the SSRT method. The strain rate was controlled at 1×10^{-6} s^{-1}. During the test, a passive potential of –0.2 V vs. SCE was adopted, which was obtained from the potentiodynamic polarization curves at slow sweep rate. In order to characterize the susceptibility qualitatively, reduction-in-area loss (I_ψ) and fracture strength loss (I_σ) were introduced to describe the toughness and strength deterioration, respectively, and were defined as

$$I_\psi = \frac{\psi_0 - \psi_E}{\psi_0} \times 100\% \quad (1)$$

$$I_\sigma = \frac{\sigma_0 - \sigma_E}{\sigma_0} \times 100\% \quad (2)$$

where ψ_E, ψ_0, σ_E, and σ_0 were corresponding to the reduction-in-area and fracture strength in solution and in air, respectively [15]. The fracture morphologies of the cross-side and surfaces of tensile specimens after the SSRT test were observed by scanning electron microscopy (SEM).

Electrochemical experiments were performed with PARSTAT 2273, using a conventional three-electrode cell system, in which a saturated calomel electrode (SCE) was used as the reference electrode and a platinum sheet as the counter electrode. All the potentials quoted in this work were referred to SCE. Prior to the test, all the electrodes were immersed in solutions until the open circuit potential (OCP) was stable. Potentiodynamic polarization curves were acquired by scanning from –1.5 to 1.5 V vs. SCE at a slow sweep rate of 1 mV/s and a quick sweep rate of 100 mV/s. EIS measurements were carried out at passive potential (if any) of –0.2 V vs. SCE, with the AC amplitude of the sinusoidal perturbation of 10 mV vs. SCE and the measurement frequency from 100 kHz to 10 mHz.

3. Results

3.1. SSRT results

The stress-strain curves of X80 pipeline steel in the solutions with different concentrations of HCO_3^- at –0.2 V vs. SCE were shown in Fig. 1. Compared with the curve obtained in air, X80 steel in bicarbonate solutions displayed susceptibility to SCC. With the increase of HCO_3^- concentration, the susceptibility enhanced with the reduction in toughness and strength, which was manifested with the elevated values of I_ψ and I_σ in Fig. 2. Among these results, it was noticed that when the concentration of HCO_3^- was relatively low (0.05 mol/L), X80 steel showed lower I_ψ and I_σ, and the fracture elongation of the specimen was almost as the same as that in air (Fig. 1), which indicated that the

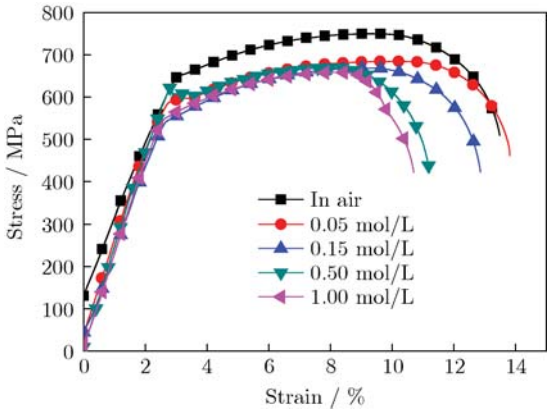

Fig. 1. Stress-strain curves of X80 steel in air and in the solutions with different concentrations of HCO_3^- at –0.2 V vs. SCE.

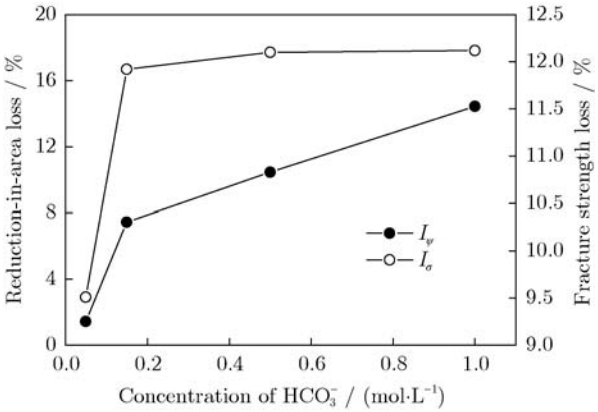

Fig. 2. Effect of HCO_3^- concentration on susceptibility to SCC reflected by reduction-in-area loss and fracture strength loss.

steel appeared little susceptibility to SCC in such a dilute bicarbonate solution. These results were further confirmed by the observation of fracture morphologies below.

3.2. Fractographic observation

In the solution containing 0.05 mol/L HCO_3^-, the steel showed little susceptibility to SCC. A densely distributed dimple feature can be found on the fracture surface (Fig. 3(a)), and there were no visible secondary cracks on the lateral surface. Moreover, the fracture surface and lateral surface were both corroded seriously due to the combined effect of a lower amount of HCO_3^- and a moderate amount of Cl^-. Considerable large and shallow pits were found on the specimen surface, and some of them were in nested type, i.e., newly formed pits evolved at the bottom of old pits (Fig. 3(b)).

When the concentration of HCO_3^- increased to 0.15 mol/L, the fractograph exhibited quasi-cleavage morphology with reduced dimples (Fig. 3(c)), and the pits were enlarged to coalesce with the adjacent ones on the lateral surface (Fig. 3(d)). With a further increase in HCO_3^- concentration, dimples continually faded and cleavage planes became more and more remarkable, showing gradually lifted brittleness (Figs. 3(e) and (g)). The formation of cleavage planes might be attributed to the rapid propagation of cracks along the slip steps until the specimen fractured. Meanwhile, the already coalesced pits grew even larger. Secondary cracks initiated at the bottom of these pits, and propagated until they were linked with the cracks emerged in the adjacent pits (Figs. 3(f) and (h)), showing a more enhanced susceptibility to SCC. Therefore, pitting probably played an important role in cracking of the steel in concentrated bicarbonate solutions.

4. Discussion

4.1. SCC mechanism of X80 steel

Potentiodynamic polarization curves measured at 1 and 100 mV/s are shown in Fig. 4. Parkins [16] pointed out that potentiodynamic polarization curves at different potential sweep rates could be used to evaluate the susceptibility to SCC of pipeline steel in some certain electrolyte environment. Scanning at a quick sweep rate would extremely eliminate the influence of the formation of passive films, guaranteeing a barely fresh metal surface exposed to the electrolyte, where intensive anodic dissolution took place, so it could reflect the electrochemical characteristic of crack tips. At the slow sweep rate for polarization, the metal surface could be sufficiently passivated, which manifested the electrochemical characteristic of non-crack tip areas.

Assuming that the SCC behavior was controlled by the anodic dissolution mechanism, it should depend on the discrepancy between corrosion rates of crack tips and non-crack tips as well as the propagation rate of crack tips [17]. The former could be represented by $i_q/i_s - 1$, and the latter could be assessed by i_q. i_q and i_s referred to the current densities at –0.2 V vs. SCE obtained from the polarization curves at quick and slow sweep rates, respectively. Thus, $i_q \cdot (i_q/i_s - 1)$ was used to estimate the susceptibility to SCC of X80 steel in different bicarbonate solutions. The calculated results of $i_q \cdot (i_q/i_s - 1)$ are shown in Fig. 5. The curve of $i_q \cdot (i_q/i_s - 1)$ varied with a same tendency as those of I_ψ and I_σ. This indicated that the higher concentration of HCO_3^- the solution contained, the higher susceptibility to SCC the steel would show. It should be noticed that the value of $i_q \cdot (i_q/i_s - 1)$ obtained in the solution containing 0.05 mol/L HCO_3^- was negative, i.e., $i_s > i_q$. Theoretically, cracking could not be initiated when the dissolution rate of non-crack tip areas was greater than that of crack tips [18]. Thus, it provided an explanation from the electrochemical kinetics aspect for the phenomenon that X80 steel exposed to dilute bicarbonate solution represented little susceptibility to SCC.

In order to estimate the reasonableness of $i_q \cdot (i_q/i_s - 1)$, the criterion of susceptibility to SCC based on electrochemical measurements [15] was introduced, which had the following form:

$$I_{SCC} = k_a \cdot i_q \cdot \left(\frac{i_q}{i_s} - 1\right) + I_a, \tag{3}$$

where k_a and I_a were constants in relation to the material/electrolyte system. By applying the results of I_ψ and I_σ, the values of k_a and I_a were estimated and the formulations used for solutions containing 0.15-1.00 mol/L HCO_3^- are given as follows:

$$I_{SCC} = \begin{cases} 1.56 \cdot i_q \cdot \left(\dfrac{i_q}{i_s} - 1\right) + 6.8\%, & \text{for } I_\psi \\ 0.044 \cdot i_q \cdot \left(\dfrac{i_q}{i_s} - 1\right) + 11.9\%, & \text{for } I_\sigma \end{cases} \tag{4}$$

The results had a good agreement with the measured results as shown in Fig. 6. It indicated that it was reasonable to use $i_q \cdot (i_q/i_s - 1)$ to evaluate the susceptibility to SCC of X80 steel at passive potential in relatively concentrated bicarbonate solutions. It also proved that the SCC behavior was controlled by the dissolution-based mechanism in these circumstances.

Thus, the cracking procedure of X80 steel in bicarbonate solutions can be expressed by Figs. 7(a)-(d). First, applied stress promoted the dislocation emission. With the accumulation of dislocations, slip bands 1 and 2 in Fig. 7(a) set in motion successively and the dislocation slip steps became more and more obvious, which led to the rupture of passive films. Dislocations were then pushed toward the slip steps and piled up there (Fig. 7(b)). When these local sites were directly exposed to the aggressive electrolytes, pitting was initiated by selective dissolution of these sites because of the relatively higher electrochemical activity

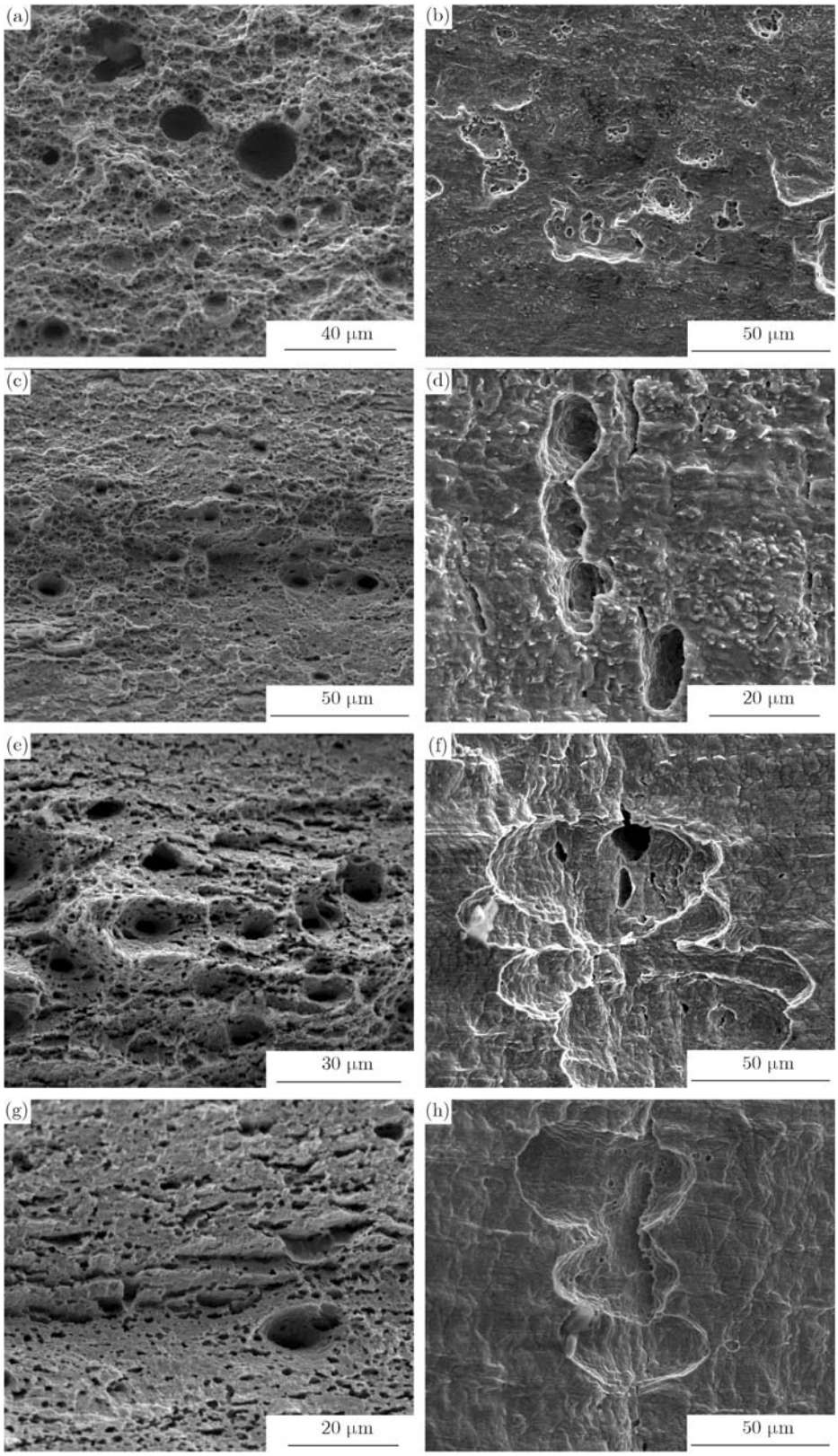

Fig. 3. Morphologies of fracture surfaces and lateral surfaces in the solutions with different concentrations of HCO_3^-: (a) fracture surface and (b) lateral surface in 0.05 mol/L bicarbonate solution; (c) fracture surface and (d) lateral surface in 0.15 mol/L bicarbonate solution; (e) fracture surface and (f) lateral surface in 0.50 mol/L bicarbonate solution; and (g) fracture surface and (h) lateral surface in 1.00 mol/L bicarbonate solution.

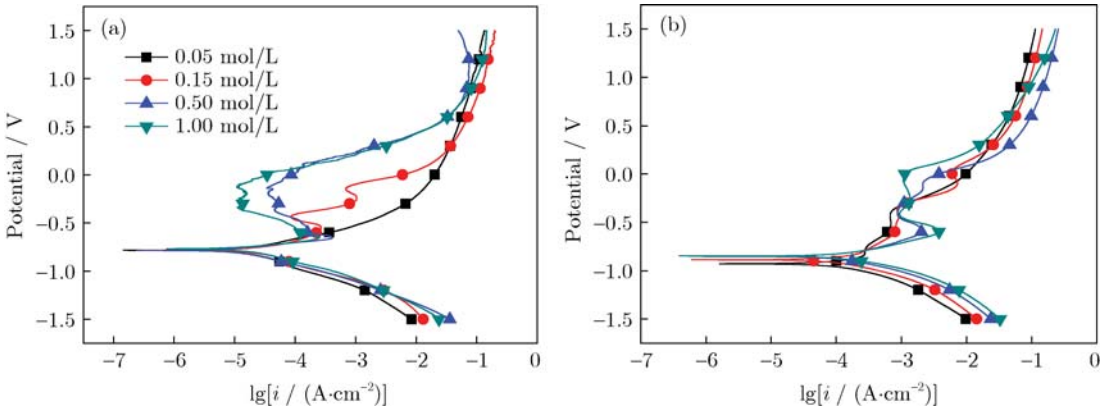

Fig. 4. Polarization curves of X80 steel in the solutions with different concentrations of HCO_3^- measured at sweep rates of 1 mV/s (a) and 100 mV/s (b).

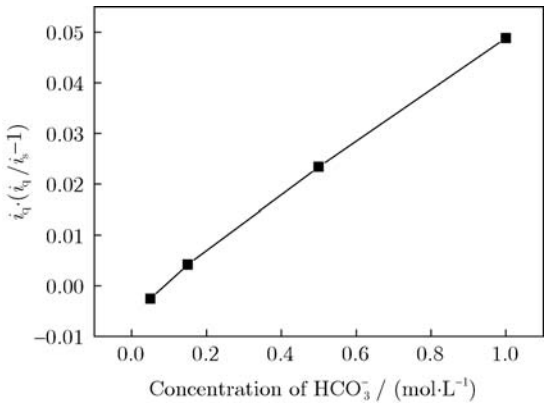

Fig. 5. Relationship between $i_q \cdot (i_q/i_s - 1)$ and HCO_3^- concentration.

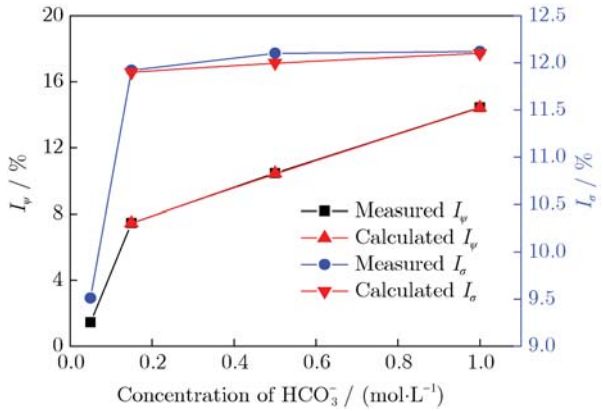

Fig. 6. Comparison between measured and calculated I_ψ and I_σ using Eq. (4).

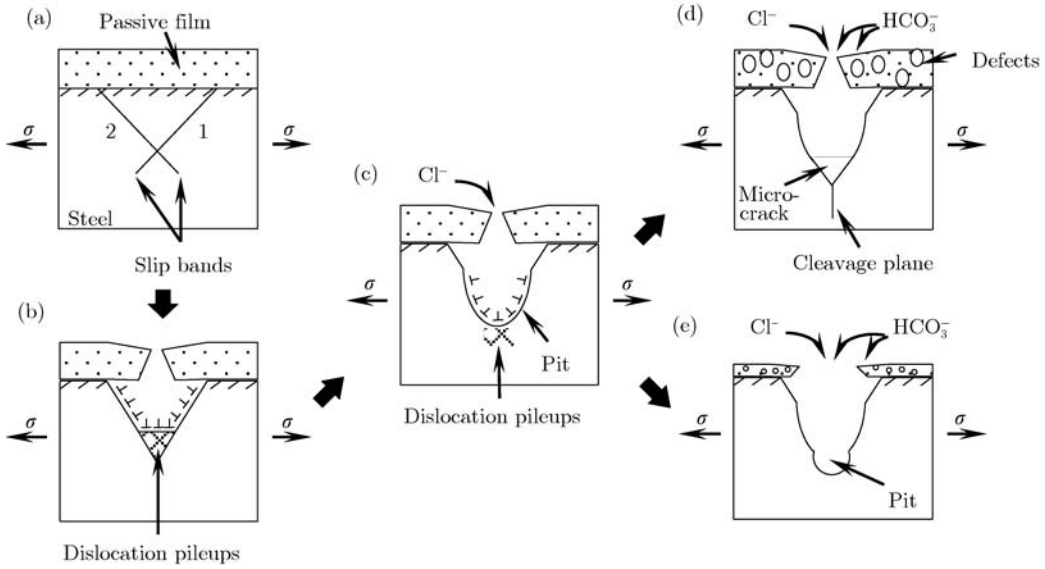

Fig. 7. Schematic diagrams showing the SCC process of X80 steel exposed to solutions containing Cl^- and different concentrations of HCO_3^-: (a) the steel with passive films in original state; (b) film rupture combined with the formation of slip steps and dislocation pileups; (c) initiation of pitting; (d) generation of defect points in passive films and cracking along cleavage planes in concentrated bicarbonate solutions; (e) development of pitting in dilute bicarbonate solution.

and lattice distortion [19]. Dislocation pileups further advanced to the bottom of these pits under the stress triaxiality (Fig. 7(c)), and the atoms at these stress concentrated points would be dissolved preferentially to form microcracks. Finally, HCO_3^- promoted the dissolution of crack tips and the propagation of cracks along cleavage planes (Fig. 7(d)). Therefore, cleavage cracks were inclined to initiate in pits formed along the dislocation slip steps as shown in Figs. 3(f) and (h).

4.2. Effect of HCO_3^- on the rupture of passive films and SCC behavior

In high pH solutions, the properties of passive films formed on the steel surface is essential to the occurrence of SCC based on the anodic dissolution mechanism [20]. Nyquist plots in Fig. 8 show that the capacitance arc corresponding to the electric double layer at high frequency decreased rapidly with the increase of HCO_3^- concentration, and the one referred to the passive films at low frequency shrank into diffusion impedance. Fig. 9 shows the equivalent electric circuit, where R_s is the resistance of the electrolyte, C_{dl} and R_{ct} correspond to the electric double layer capacitance and charge transfer resistance, respectively, and W is the Warburg impedance. By using the equivalent electric circuit in Fig. 9, the fitting values of R_{ct} are shown in Fig. 10. R_{ct} decreased with an increase in HCO_3^- concentration, indicating that the inhibiting effect of passive films on the diffusion of aggressive electrolytes was deteriorated by excessive HCO_3^-.

Davies and Burstein [21] pointed out that HCO_3^- could accelerate the dissolution of the steels whether in the active or in passive potential region due to the formation of soluble composite ion $Fe(CO_3)_2^{2-}$:

$$FeCO_3 + HCO_3^- \rightarrow Fe(CO_3)_2^{2-} + H^+. \quad (5)$$

The initially formed passive films were dissolved by excessive HCO_3^- in accordance with Eq. (5). As a result, the transformation of the passive films from $FeCO_3$ to more stable phase Fe_3O_4 and Fe_2O_3 at –0.2 V vs. SCE was suppressed. Subsequently, pores and other type of defects in the passive films increased [22]. These defects made the absorption points and penetration path formed for the aggressive ions (Cl^- and HCO_3^-), which facilitated the rupture of passive films, as well as the occurrence of pitting and cracking at these locations [23] as shown in Fig. 7(d). Moreover, the increase of HCO_3^- concentration could promote the anodic dissolution of crack tips [12], which is represented with the rapid increase of $i_q \cdot (i_q/i_s - 1)$ as shown in Fig. 5. That is why higher concentrations of HCO_3^- contributed to a higher susceptibility to SCC of X80 steel.

However, X80 steel showed little susceptibility to SCC in dilute bicarbonate solution (0.05 mol/L HCO_3^-). The initiation of SCC can be seen as a competition procedure between the rupture and the repassivation of passive films, in which only moderate repassivation rate is beneficial to cracking [24]. In this work, the steel could not be passivated in this dilute solution as shown in Fig. 4(a), and the value of $i_q \cdot (i_q/i_s - 1)$ was below zero (Fig. 5), i.e., i_s was greater than i_q at –0.2 V vs. SCE, so the formation of passive films at crack tips and in non-crack tip areas were both inhibited, and the non-crack tip areas experienced relatively more intensive dissolution than the crack tips. It can be concluded that the repassivation of passive films significantly fell behind the rupture in this circumstance. Therefore, microcracks, once emerged, would not propagate but instantly go blunt and transform into pits because of intensive dissolution at the sidewalls of the cracks. After that, new microcracks initiated and devel-

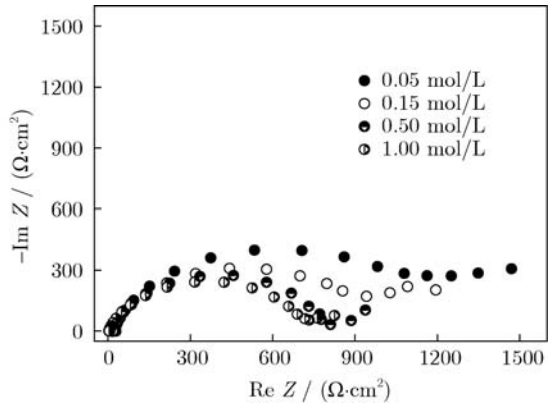

Fig. 8. EIS plots of X80 steel in the solutions with different concentrations of HCO_3^- at –0.2 V vs. SCE.

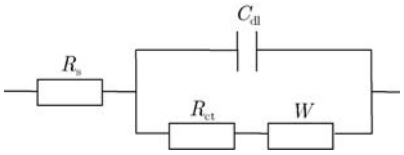

Fig. 9. Equivalent electric circuit.

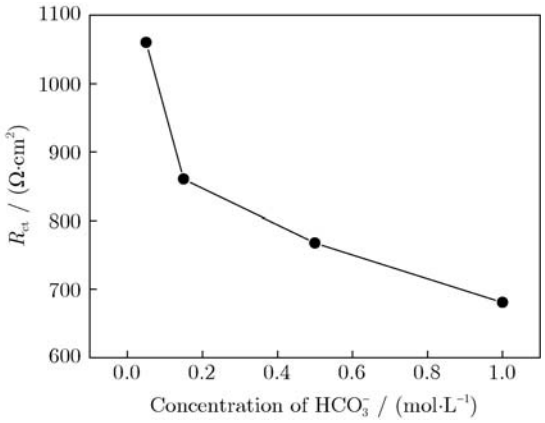

Fig. 10. Relationship between R_{ct} and HCO_3^- concentration.

oped into new pits at the bottom of the original pits. Consequently, only the development of pitting was observed as shown in Fig. 3(b). The schematic diagram related to this process is shown in Fig. 7(e). Therefore, the tendency to SCC caused by the dissolution-based mechanism was negligible in dilute bicarbonate solution.

5. Conclusions

(1) It is proven that the SCC behavior of X80 steel at –0.2 V vs. SCE in concentrated bicarbonate solutions containing 0.15-1.00 mol/L HCO_3^- is controlled by the dissolution-based mechanism, and the susceptibility to SCC can be evaluated by using $i_q \cdot (i_q/i_s - 1)$. The increase in HCO_3^- concentration results in the enhanced susceptibility to SCC. Cleavage cracks are inclined to initiate in pits formed along the dislocation slip steps.

(2) The rupture of passive films is promoted by excessive HCO_3^-, which also facilitates the occurrence of pitting and cracking. Increasing the HCO_3^- concentration not only increases the number of defects in passive films due to the formation of the soluble composite ion $Fe(CO_3)_2^{2-}$ but also promotes the anodic dissolution of crack tips.

(3) X80 steel only shows the development of pitting at –0.2 V vs. SCE in dilute bicarbonate solution with 0.05 mol/L HCO_3^-, and the tendency to SCC caused by anodic dissolution can be negligible. This should be attributed to the inhibited repassivation process, manifesting as the more intensive dissolution in the non-crack tip areas than at the crack tips.

References

[1] L. Zhang, X.G. Li, C.W. Du, and Y.Z. Huang, Effect of applied potentials on stress corrosion cracking of X70 pipeline steel in alkali solution, *Mater. Des.*, 30(2009), No. 6, p. 2259.

[2] C.F. Dong, K. Xiao, Z.Y. Liu, W.J. Yang, and X.G. Li, Hydrogen induced cracking of X80 pipeline steel, *Int. J. Miner. Metall. Mater.*, 17(2010), No. 5, p. 579.

[3] G. Van Boven, W. Chen, and R. Rogge, The role of residual stress in neutral pH stress corrosion cracking of pipeline steels: Part I. Pitting and cracking occurrence, *Acta Mater.*, 55(2007), No. 1, p. 29.

[4] B.T. Lu, F. Song, M. Gao, and M. Elboujdaini, Crack growth model for pipelines exposed to concentrated carbonate-bicarbonate solution with high pH, *Corros. Sci.*, 52(2010), No. 12, p. 4064.

[5] G.A. Zhang and Y.F. Cheng, Micro-electrochemical characterization and Mott-Schottky analysis of corrosion of welded X70 pipeline steel in carbonate/bicarbonate solution, *Electrochim. Acta*, 55(2009), No. 1, p. 316.

[6] T. Li, Y.J. Yang, K.W. Gao, and M.X. Lu, Mechanism of protective film formation during CO_2 corrosion of X65 pipeline steel, *J. Univ. Sci. Technol. Beijing*, 15(2008), No. 6, p. 702.

[7] L.N. Xu, H.M. Qin, W. Chang, L. Zhang, M.X. Lu, and S.F. Li, CO_2 corrosion behavior of X70 pipeline steel in wet gas environment, *J. Univ. Sci. Technol. Beijing*, 33(2011), No. 12, p. 1478.

[8] A.Q. Fu and Y.F. Cheng, Electrochemical polarization behavior of X70 steel in thin carbonate/bicarbonate solution layers trapped under a disbonded coating and its implication on pipeline SCC, *Corros. Sci.*, 52(2010), No. 7, p. 2511.

[9] P. Liang, C.W. Du, X.G. Li, X. Chen, and L. Zhang, Effect of hydrogen on the stress corrosion cracking behavior of X80 pipeline steel in Ku'erle soil simulated solution, *Int. J. Miner. Metall. Mater.*, 16(2009), No. 4, p. 407.

[10] P. Liang, X.G. Li, C.W. Du, X. Chen, and L. Zhang, Influence of chloride ions on the corrosion resistance of X80 pipeline steel in $NaHCO_3$ solution, *J. Univ. Sci. Technol. Beijing*, 30(2008), No. 7, p. 735.

[11] A. Eslami, R. Kania, B. Worthingham, G.V. Boven, R. Eadie, and W. Chen, Effect of CO_2 and *R*-ratio on near-neutral pH stress corrosion cracking initiation under a disbonded coating of pipeline steel, *Corros. Sci.*, 53(2011), No. 6, p. 2318.

[12] R.N. Parkins and S. Zhou, The stress corrosion cracking of C-Mn steel in CO_2-HCO_3^--CO_3^{2-} solutions: II. Electrochemical and other data, *Corros. Sci.*, 39(1997), No. 1, p. 175.

[13] L. Fan, X.G. Li, C.W. Du, and Z.Y. Liu, Electrochemical behavior of passive films formed on X80 pipeline steel in various concentrated $NaHCO_3$ solutions, *J. Chin. Soc. Corros. Prot.*, 32(2012), No. 4, p. 322.

[14] J.L. Zhou, X.G. Li, C.W. Du, Y. Pan, T. Li, and Q. Liu, Passivation process of X80 pipeline steel in bicarbonate solutions, *Int. J. Miner. Metall. Mater.*, 18(2011), No. 2, p. 178.

[15] Z.Y. Liu, X.G. Li, C.W. Du, G.L. Zhai, and Y.F. Cheng, Stress corrosion cracking behavior of X70 pipe steel in an acidic soil environment, *Corros. Sci.*, 50(2008), No. 8, p. 2251.

[16] R.N. Parkins, Predictive approaches to stress corrosion cracking failure, *Corros. Sci.*, 20(1980), No. 2, p. 147.

[17] R.N. Parkins, Mechanistic aspects of intergranular stress corrosion cracking of ferritic steels, *Corrosion*, 52(1996), No. 5, p. 363.

[18] Z.Y. Liu, X.G. Li, Y.R. Zhang, C.W. Du, and G.L. Zhai, Relationship between electrochemical characteristics and SCC of X70 pipeline steel in an acidic soil simulated solution, *Acta Metall. Sin. Engl. Lett.*, 22(2009), No. 1, p. 58.

[19] D. Li, F.Y. Meng, X.Q. Ma, L.J. Qiao, and W.Y. Chu, Molecular dynamics simulation of porous layer-induced stress in Fe single crystal, *Comput. Mater. Sci.*, 49(2010), No. 3, p. 641.

[20] R.N. Parkins, W.K. Blanchard Jr., and B.S. Delanty,

Transgranular stress corrosion cracking of high-pressure pipelines in contact with solutions of near neutral pH, *Corrosion*, 50(1994), No. 5, p. 394.

[21] D.H. Davies and G.T. Burstein, The effects of bicarbonate on the corrosion and passivation of iron, *Corrosion*, 36(1980), No. 8, p. 416.

[22] G.Z. Meng, C. Zhang, and Y.F. Cheng, Effects of corrosion product deposit on the subsequent cathodic and anodic reactions of X-70 steel in near-neutral pH solution, *Corros. Sci.*, 50(2008), No. 11, p. 3116.

[23] P. Liang, X.G. Li, C.W. Du, and X. Chen, Stress corrosion cracking of X80 pipeline steel in simulated alkaline soil solution, *Mater. Des.*, 30(2009), No. 5, p. 1712.

[24] J.Q. Wang and A. Atrens, SCC initiation for X65 pipeline steel in the "high" pH carbonate/bicarbonate solution, *Corros. Sci.*, 45(2003), No. 10, p. 2199.